Microbiological Research 171 (2015) 26–31

Contents lists available at ScienceDirect

Microbiological Research

journal homepage: www.elsevier.com/locate/micres

Glycine metabolism and anti-oxidative defence mechanisms in *Pseudomonas fluorescens*

Azhar Alhasawi, Zachary Castonguay, Nishma D. Appanna, Christopher Auger, Vasu D. Appanna*

Faculty of Science and Engineering, Laurentian University, Sudbury, ON, Canada

ARTICLE INFO

Article history:
Received 19 October 2014
Received in revised form
25 November 2014
Accepted 7 December 2014
Available online 6 January 2015

Keywords:
Oxidative stress
Metabolism
Glyoxylate
Antioxidant
ATP

ABSTRACT

The role of metabolism in anti-oxidative defence is only now beginning to emerge. Here, we show that the nutritionally-versatile microbe, *Pseudomonas fluorescens*, reconfigures its metabolism in an effort to generate NADPH, ATP and glyoxylate in order to fend off oxidative stress. Glyoxylate was produced predominantly via the enhanced activities of glycine dehydrogenase-$NADP^+$ (GDH), glycine transaminase (GTA) and isocitrate lyase (ICL) in a medium exposed to hydrogen peroxide (H_2O_2). This ketoacid was utilized to produce ATP by substrate-level phosphorylation and to neutralize reactive oxygen species with the concomitant formation of formate. The latter was also a source of NADPH, a process mediated by formate dehydrogenase-$NADP^+$ (FDH). The increased activities of phosphoenolpyruvate carboxylase (PEPC) and pyruvate orthophosphate dikinase (PPDK) worked in tandem to synthesize ATP in the H_2O_2-challenged cells that had markedly diminished capacity for oxidative phosphorylation. These metabolic networks provide an effective means of combating ROS and reveal therapeutic targets against microbes resistant to oxidative stress.

Introduction

All aerobic organisms are exposed to oxidative stress and have evolved intricate mechanisms to combat the dangers posed by reactive oxygen species (ROS) (Groves and Lucana 2010). While catalase is involved in the detoxification of hydrogen peroxide (H_2O_2), superoxide dismutase helps neutralize the toxicity of superoxide (O_2^-) (Zeller and Klug 2004; Bruno-Bárcena et al. 2010). Glutathione peroxidase is another enzyme involved in the removal of H_2O_2 with the aid of the tripeptide glutathione (Sato et al. 2009). The sulphydryl group in glutathione is key in maintaining a reductive environment (Jozefczak et al. 2012). However, it is critical to generate reduced glutathione once it has been oxidized. This is achieved with the participation of the enzyme glutathione reductase and its cofactor, reduced nicotinamide adenine dinucleotide phosphate (NADPH) (Masip et al. 2006).

NADPH-generating enzymes also constitute an important strategy in the elimination of oxidative stress. Glucose-6-phosphate dehydrogenase, malic enzyme, $NADP^+$-dependent isocitrate dehydrogenase, $NADP^+$-dependent glutamate dehydrogenase and nicotinamide adenine dinucleotide kinase (NADK) are some of players that help orchestrate an adequate supply of NADPH (Singh et al. 2008; Sandoval et al. 2011). The role of ketoacids in countering the oxidative burden has only recently begun to be appreciated (Lemire et al. 2010). Ketoacids react with ROS with the concomitant formation of the corresponding carboxylic acid and CO_2. For instance, pyruvate neutralizes H_2O_2 while forming acetate by non-enzymatic decarboxylation; αKG detoxifies ROS, succinate is produced as a by-product (Bignucolo et al. 2013). The latter has been shown to play an important role in signalling processes (Tannahill et al. 2013). Hence, metabolic networks aimed at fine-tuning the levels of ketoacids are also emerging as a potent tool in the antioxidant armoury of numerous organisms (Kohen and Nyska 2002; Li et al. 2010).

As part of our study to decipher the role of ketoacids in anti-oxidative defense, we have investigated the ability of *Pseudomonas fluorescens* to survive an oxidative challenge in a mineral medium containing glycine as the source of nitrogen. The metabolism of glycine to the ketoacid, glyoxylate and its involvement in combating oxidative stress has been examined. The role of NADPH-generating enzymes and alternative ATP-producing pathways are also discussed.

* Corresponding author. Tel.: +1 705 675 1151x2112.
E-mail address: vappanna@laurentian.ca (V.D. Appanna).

http://dx.doi.org/10.1016/j.micres.2014.12.001
0944-5013/

Materials and methods

Conditions of growth

P. fluorescens (ATCC 13525), obtained from American type culture collection was grown in a defined glycine/citrate media consisting of Na_2HPO_4 (6 g), KH_2PO_4 (3 g), 15 mM glycine (1.2 g), $MgSO_4{\cdot}7H_2O$ (0.2 g), 19 mM citrate (4 g). Trace elements were added as previously described in (Mailloux et al. 2008). ROS stress was induced via the addition of 500 μM H_2O_2 to the media prior to the inoculation of *P. fluorescens*. A second dose of H_2O_2 was introduced 24 hours after the initial amount in order to maintain a constant level of ROS in the system. The pH of the media was adjusted to 6.8 using dilute NaOH and dispensed into 200 mL aliquots in 500 mL Erlenmeyer flasks. The medium was autoclaved for 20 min at 121 °C and inoculated using 1 mL of *P. fluorescens* grown to the stationary phase in the control medium. Cultures were aerated in a gyratory water bath shaker, model 76 (New Brunswick Scientific) at 26 °C at 140 rpm. The cells and spent fluid were isolated at the stationary phase of growth for metabolomic and enzymatic analyses (28 h for the control, and 50 h growth for the H_2O_2 stressed cultures ensured similar growth phases). Cell growth was monitored by measuring the solubilized protein contents by the Bradford assay (Bradford 1976).

Cellular fractionation

Bacteria were collected at similar stages of growth and resuspended in 500 μL cell storage buffer (CSB) consisting of 50 mM Tris–HCl, 5 mM $MgCl_2$ and 1 mM phenylmethylsulphonyl fluoride (PMSF). These were lysed via sonication and centrifuged at 180,000 × *g* for 3 h at 4 °C yielding a soluble fraction, and a membrane fraction. The membrane fraction was suspended in 500 μL of CSB. The protein content in the soluble and membrane fractions were determined using the Bradford assay (Bradford 1976).

Metabolite analysis

Metabolite levels were examined using HPLC. Cells were grown in control and H_2O_2-stressed conditions and isolated at similar growth phases and homogenized via sonication as described previously, yielding cell free extract (CFE) and supernatant. The CFE was boiled for 10 min to precipitate proteins before analysis. Samples of CFE and spent fluid were injected into an Alliance HPLC equipped with a C18 reverse-phase column (Synergi Hydro-RP; 4 μm; 250 mm × 4.6 mm, Phenomenex) operating at a flow rate of 0.2 mL/min at ambient temperature. A mobile phase consisting of 20 mM K_2HPO_4 (pH 2.9) was used to separate organic acids, which were detected using a Waters dual absorbance detector at 210 nm. Metabolites were identified using known standards, and peaks were quantified with the aid of the Empower software (Waters Corporation) (Alhasawi et al. 2014).

BN PAGE in-gel activity

Blue native (BN) polyacrylamide gel electropohoresis (PAGE) was performed following a modified method described previously (Mailloux et al. 2005). Membrane and cytosolic fractions that were isolated were prepared in a non-denaturing buffer (50 mM Bis–Tris, 500 mM ε-aminocaproic acid, pH 7.0, 4 °C) at a concentration of 4 μg/μL. Ten percent maltoside was added to membrane fractions to help solubilize membrane bound proteins. A 4–16% gradient gel was prepared with the Bio-Rad MiniProteanTM 2 system using 1 mm spacers to ensure optimal protein separation. Sixty micrograms of protein were loaded into each well and electrophoresed under native conditions at 80 V to ensure proper stacking, then at 300 V for proper migration through the gel. The blue cathode buffer (50 mM Tricine, 15 min Bis–Tris, 0.02% (w/v) Coomassie G-250 (pH 7) at 4 °C) was used to help visualize the running front and was changed to a colourless cathode buffer (50 mM Tricine, 15 mM Bis–Tris, pH 7 at 4 °C) when the running front was halfway through the gel. Upon completion the gel was equilibrated in reaction buffer for 15–30 min. The in-gel visualization of enzyme activity was ascertained by coupling the formation of NAD(P)H to 0.3 mg/mL of phenazine methosulfate (PMS) and 0.5 mg/mL of iodonitrotetrazolium (INT), or by coupling the formation of $NAD(P)^+$ to 16.7 μg/mL DCPIP and 0.5 mg/mL INT. Complex 1 was detected by the addition of 5 mM NADH, and 0.4 mg/mL INT. Isocitrate dehydrogenase (ICDH-NADP) activity was visualized using a reaction mixture containing 5 mM isocitrate, 0.5 mM $NADP^+$ or NAD^+, 0.2 mg/mL PMS and 0.4 mg/mL INT. Glycine dehydrogenase (GDH) activity was visualized using a reaction mixture consisting of reaction buffer, 5 mM glycine, 0.5 mM $NADP^+$ or NAD^+, 0.4 mg/mL INT and 0.2 mg/mL PMS. Glycine transaminase (GTA) activity was visualized using a reaction mixture consisting of reaction buffer, 10 mM glycine, 0.5 mM NAD^+, 5 mM α-ketoglutarate, 5 units of glutamate dehydrogenase, 0.4 mg/mL INT and 0.2 mg/mL PMS. Acylating glyoxylate dehydrogenase (AGODH) activity was visualized using a reaction mixture consisting of reaction buffer, 5 mM glyoxylate, 0.83 mM $NADP^+$, 0.66 mM coenzyme A, 0.4 mg/mL INT, and 0.2 mg/mL PMS. PEPC and PPDK activities were visualized as described previously (Alhasawi et al. 2014). Malate dehydrogenase (MDH) and isocitrate lyase (ICL) activities were visualized as described (Hamel et al. 2004; Singh et al. 2005). $NAD(P)^+$-dependent formate dehydrogenase was monitored using a reaction mixture containing reaction buffer, 5 mM formate, 0.5 mM NAD^+ or $NADP^+$, 0.4 mg/mL INT, 0.2 mg/mL PMS.

Reactions were stopped using a destaining solution (40% methanol, 10% glacial acetic acid) once the activity bands had reached the desired intensity. Reactions performed without the addition of a substrate or cofactor in the reaction mixture ensured specificity. Densitometry was performed using ImageJ for Windows. Spectrophotometric data for ICDH-NAD was obtained by incubating 1 mg of membrane CFE from control and H_2O_2-treated cells with 2 mM isocitrate and 0.5 mM NAD^+ of 1 min. A similar mixture was used for MDH, but isocitrate was replaced with malate. NADH production was monitored at 340 nm. For pyruvate carboxylase (PC) analysis, the membrane CFE was given 2 mM pyruvate, 0.5 mM ATP, 0.5 mM HCO_3^-, 10 units of MDH and 0.5 mM NADH. The disappearance of NADH was monitored at 340 nm over the course of 1 min. Negative controls were performed without the substrates or cofactors.

Regulation experiments

The regulation of GDH and GTA in response to H_2O_2 was examined as follows. Two cultures were grown to the similar growth phase as described previously, the stressed cells were then inoculated into control media, and the control cells were inoculated into a medium with 500 μM H_2O_2. Cells were allowed to grow for 4 h and then isolated as described before. GDH and GTA activity levels were probed.

Results

When *P. fluorescens* was subjected to H_2O_2 challenge in medium with glycine as the sole source of nitrogen, the microbe experienced a slower rate of growth than in the control culture. In the latter the stationary phase of growth was attained at 28 h of incubation while in the medium exposed to the oxidative stress, the stationary phase of growth was observed at 50 h (Fig. 1A). However, there was no

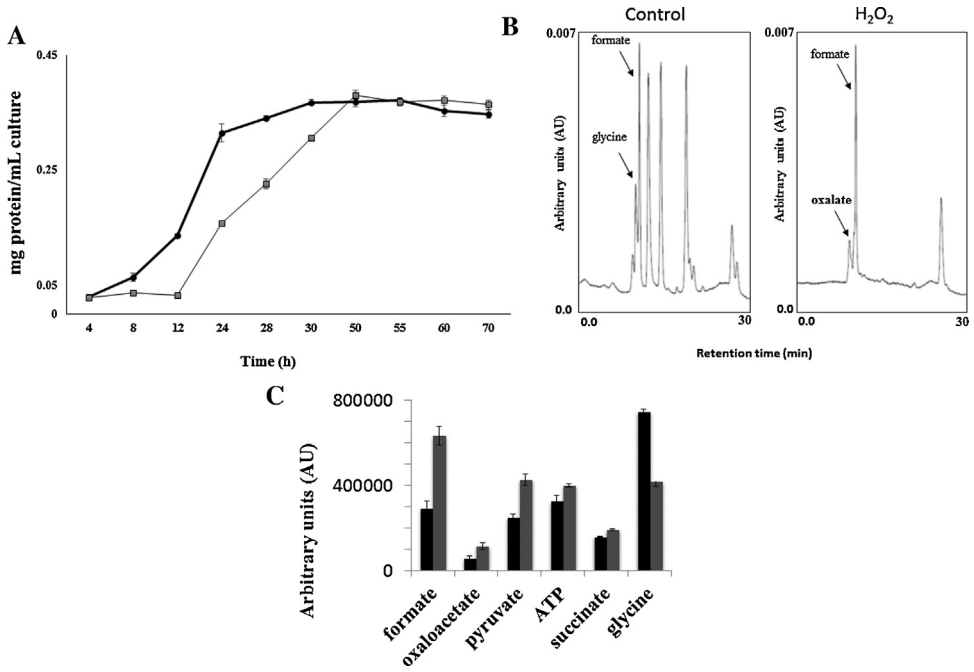

Fig. 1. (A) Cellular yield of *P. fluorescens* in control (●) and 500uM H_2O_2-treated ( ) samples, as measured by the Bradford assay (B) Metabolite profiles in the spent fluid from control and H_2O_2-treated *P. fluorescens* (Representative chromatogram; $n = 3$). (C) Metabolite profile from the soluble cell free extract of control ( ) and H_2O_2-treated (■) cells ($n = 3$).

discernable variation in cellular yield. The spent fluid from the stressed cultures contained higher levels of oxalate while a strong glycine peak was evident in the spent fluid from control cultures (Fig. 1B). There was also a noticeable difference in the metabolites isolated from the CFE obtained from the stressed cultures compared to the control. Peaks attributable to ATP, pyruvate, succinate, oxaloacetate and formate were more prominent (Fig. 1C).

In an effort to identify the metabolic pathways utilized to form glyoxylate, various enzymes involved in synthesis of this ketoacid were monitored. Glycine dehydrogenase (GDH), an enzyme that mediates the formation of glyoxylate and ammonia in the presence of either NAD^+ or $NADP^+$ was found to be up-regulated in activity in the stressed cells (Fig. 2A). The activity of glycine transaminase (GTA), an enzyme that effects the transamination reaction involving αKG was also increased in the H_2O_2-challenged cells (Fig. 2B). Glycine deaminase was not detected in these cultures (data not shown). As citrate was the other carbon source in this study, the enzyme isocitrate lyase (ICL) involved in the generation of glyoxylate and succinate was monitored. The activity of ICL was indeed higher in the stressed culture compared to the control (Fig. 2C). These enzymatic changes were due to the oxidative stress as these observations were reversed when the stressed cells were incubated in a control medium and control cultures in a H_2O_2 medium. Both the activities of GDH and GTA that were sharply increased in the stressed cultures underwent a marked reduction in the control cultures (Fig. 2D). The elevated level of formate indicated that glyoxylate was a precursor of this carboxylic acid. Glyoxylate is known to generate formate upon treatment with H_2O_2 (Grodzinski and Butt 1976). Indeed, *in vitro* experiments did reveal the appearance of a formate peak with the concomitant diminution of glyoxylate upon addition of H_2O_2 (Fig. 3A). Enzymes like ICDH-NAD and αKGDH that participate in the TCA cycle were sharply diminished in the stressed cultures as were the activities of the enzymes involved in the electron transport chain (ETC) (Fig. 3B). Complex I was two-fold lower in activity in the stressed cells (Fig. 3C). The production of NADPH, a moiety that helps maintain the cellular reductive potential, was enhanced via the increased activity of ICDH-NADP, FDH-NADP, and AGODH (Fig. 3D). The latter enzyme has a dual role of producing NADPH and generating oxalyl-CoA that is eventually tapped as a source of ATP. The activity of glucose-6-phosphate dehydrogenase, a primary generator of NADPH in the pentose phosphate pathway, was also up-regulated (data not shown). PEPC and PPDK that were involved in producing ATP by substrate-level phosphorylation were also activated in the cells exposed to H_2O_2 (Fig. 4A). The former helps convert oxaloacetate into phosphoenolpyruvate (PEP) while the latter utilizes AMP to generate ATP from PEP. MDH was analyzed to determine how oxaloacetate was being generated to drive the activity of PEPC, and this enzyme was indeed up-regulated in the stressed cells (Fig. 4B) There was no significant variation in pyruvate carboxylase (PC) in the control cells compared to the H_2O_2 challenged bacteria (Fig. 4C). Select enzymes were confirmed via spectrophotometric assays. While the activities of ICDH-NAD were markedly higher in the control culture, the activity of PC was relatively similar (Table 1).

Table 1
Various enzymatic activities in cell-free extracts from control and H_2O_2-stressed bacteria at the same growth phase as monitored via spectrophotometry.

Enzyme name	Control	H_2O_2-treated
NAD^+-dependent isocitrate dehydrogenase[a]	0.88 ± 0.09	0.39 ± 0.05
Malate dehydrogenase[a]	0.48 ± 0.07	0.75 ± 0.03
Pyruvate carboxylase[b]	0.97 ± 0.08	1.03 ± 0.07

[a] μmol NADH produced min^{-1} mg $protein^{-1}$ as monitored at 340 nm ($n = 3 \pm$ standard deviation).
[b] μmol NADH consumed min^{-1} mg $protein^{-1}$ as monitored at 340 nm ($n = 3 \pm$ standard deviation).

Discussion

The foregoing data point to a critical role of metabolism in the survival of *P. fluorescens* exposed to oxidative stress. The metabolic shift evoked to combat ROS involves the production of three metabolites, ATP, NADPH and glyoxylate, which are critical to neutralizing this toxin. The need of this ketoacid in the adaptation process is so pivotal that it is generated via three enzymes with

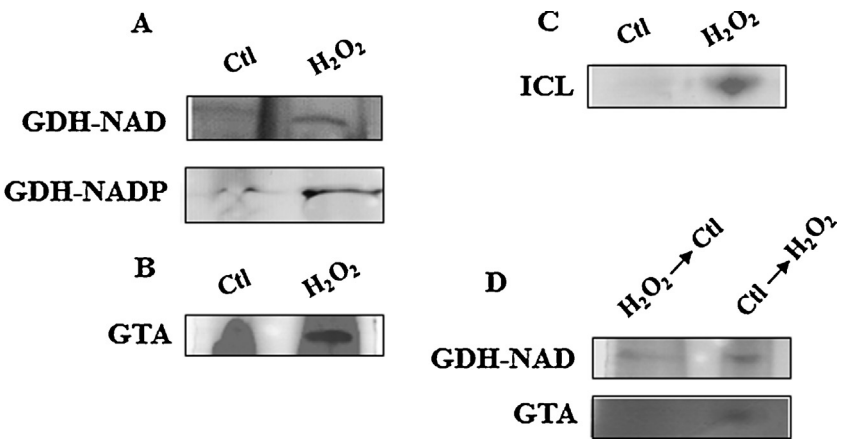

Fig. 2. (A) In-gel activity of NAD(P)$^+$-dependent glycine dehydrogenase (GDH) measured following BN-PAGE. (B) In-gel activity of glycine transaminase (GTA). (C) In-gel activity of isocitrate lyase. (D) In-gel activity of GDH-NAD and GTA following regulation experiments. Gels are representative of 3 independent experiments. Ctl, Control; H_2O_2-treated.

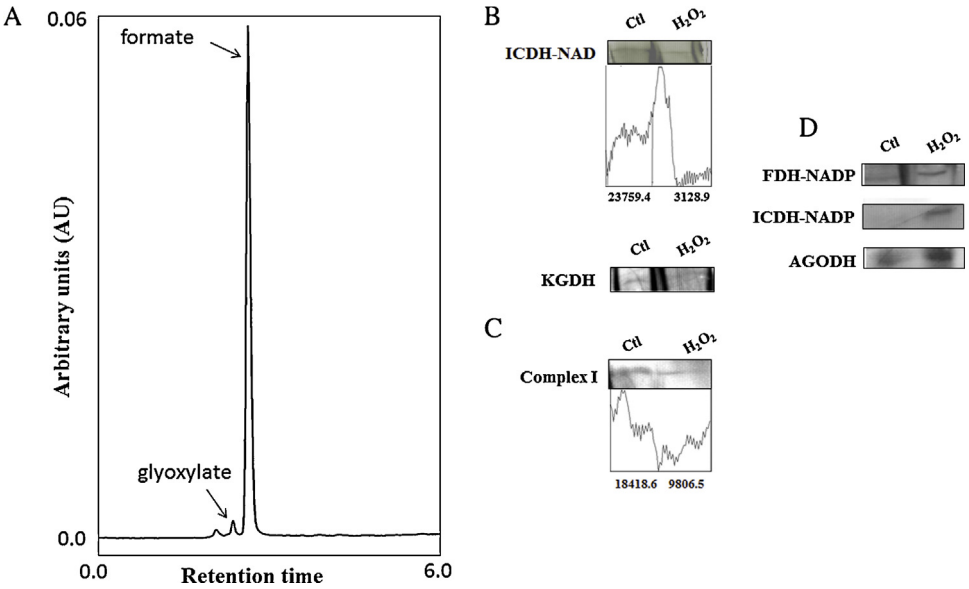

Fig. 3. (A) HPLC measurement of formate following the reaction of mM glyoxylate and mM H_2O_2. (B) In-gel activity of NAD$^+$-dependent isocitrate dehydrogenase (ICDH) and α-ketoglutarate dehydrogenase (KGDH) measured following BN-PAGE. (C) In-gel activity of complex I. (D) In-gel activity of NADP$^+$-dependent formate dehydrogenase (FDH), ICDH-NADP and acylating glyoxylate dehydrogenase (AGODH). Gels are representative of 3 independent experiments. Ctl, Control; H_2O_2-treated. Densitometry was performed using ImageJ for Windows.

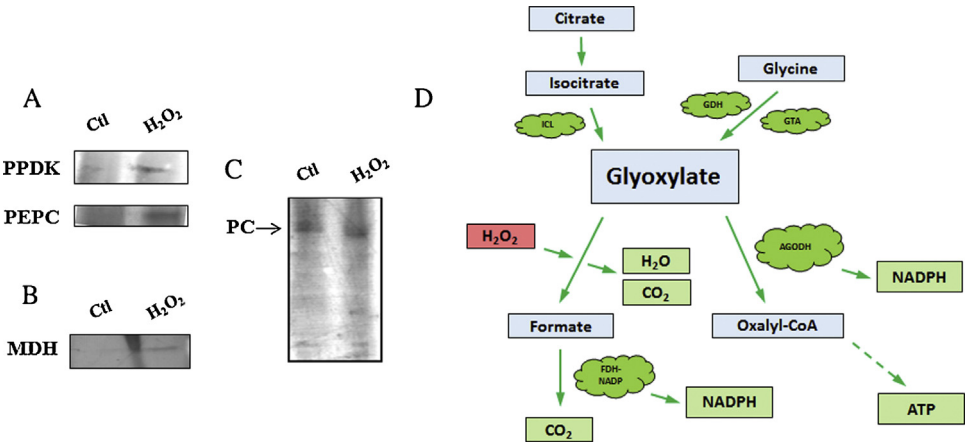

Fig. 4. (A) In-gel activity of pyruvate orthophosphate dikinase (PPDK) and phosphoenolpyruvate carboxylase (PEPC) measured following BN-PAGE. (B) In-gel activity of malate dehydrogenase (MDH). (C) In-gel activity of pyruvate carboxylase (PC). Gels are representative of 3 independent experiments. Ctl, Control; H_2O_2-treated. (D) Scheme demonstrating the glycine-based metabolic networks used to combat oxidative stress in *P. fluorescens*.

enhanced activities in the H_2O_2-challenged cultures. The activity of GDH-NADP, GTA and ICL were all numerous fold higher compared to control cultures. The formation of glyoxylate mediated by these metabolic networks appears to have the dual benefit of producing the reducing agent NADPH and the universal energy currency ATP (Beriault et al. 2007).

While the ability of ketoacids to scavenge ROS has long been known (Hofrichter et al. 1998), their precise role as antioxidants in biological systems is only now beginning to emerge (Lemire and Appanna 2011). Ketoacids can detoxify ROS with the concomitant formation of the corresponding carboxylic acid and CO_2. For instance, when αKG participates as an ROS scavenger, succinate is produced (Lemire and Appanna 2011; Mailloux et al. 2008). The involvement of pyruvate and oxaloacetate as antioxidants helps liberate acetate and malonate respectively (Campos et al. 2012; Ramsey et al. 2014). These carboxylic acids may also signal anaerobiosis. Ketoacids are important constituents of metabolic pathways that are usually part of the energy-generating machinery of the cell as they tend to supply reducing factors such as NADH. However, the latter is known as a pro-oxidant and its continued formation exacerbates the oxidative stress (Ying 2008). Hence, the diversion of ketoacids not only helps detoxify ROS but also decreases oxidative stress by limiting the synthesis of NADH (Somerville and Proctor 2009; Sharma et al. 2012). Neutralizing ROS without quelling its production may prove onerous to the organism. Thus, involving ketoacids as antioxidants may provide an effective remedy by both eliminating and inhibiting the formation of ROS. Glyoxylate appears to be a potent antioxidant as it generates formate following its interaction with a ROS (Yokota et al. 1983, 1985). This carboxylic acid can readily act as a reducing factor and can also help generate NADPH, a process mediated by formate dehydrogenase.

The presence of $NADP^+$-dependent glycine dehydrogenase (GDH) in the stressed cultures may also help contribute to the reduction of oxidative stress. NADPH is a key effector of cellular reductive potential (Mailloux et al. 2007, 2011) ICDH-NADP was another NADPH-generating enzyme with increased activity. The up-regulation in the activities of ICL and ICDH-NADP is known to counteract the ineffective aconitase in oxidatively challenged cells (Mailloux et al. 2011). In Al-stressed cultures, the metabolism of citrate is rendered possible due to these two isocitrate-degrading enzymes (Appanna et al. 2003; Hamel et al. 2004). As the machinery involved in oxidative phosphorylation is severely impeded by the H_2O_2 challenge, *P. fluorescens* utilizes substrate level phosphorylation (SLP) to satisfy its ATP need. The acylating glyoxylate dehydrogenase mediates the formation of both NADPH and oxalyl-CoA. The latter adds to the ATP budget with the concomitant formation of oxalate. This dicarboylic acid is also known as an ROS scavenger (Habibzadegah-Tari et al. 2006; Ezaki et al. 2000). Indeed, numerous organisms are known to up-regulate the synthesis of oxalate under stress. Oxalate can also chelate metals, a feature that may also help alleviate oxidative tension (Singh et al. 2008; Hamel et al. 2004). PEPC and PPDK are two enzymes that work in tandem to generate ATP in a manner independent of oxygen (Alhasawi et al. 2014). In this instance, the PEP produced by PEPC is transformed into ATP with the aid of PPDK. The involvement of AMP instead of ADP adds to the energy budget of the cell (Varela-Gomez et al. 2004).

In conclusion, *P. fluorescens* survives oxidative stress by up-regulating the production of glyoxylate, NADPH and ATP. Glyoxylate also acts as an antioxidant while NADPH helps decrease the cellular oxidative tension. The generation of ATP via SLP limits ROS production and allows the organism to proliferate despite the ineffectiveness of the energy-producing system dependent on oxidative phosphorylation (Fig. 4D). The involvement of ketoacids in mitigating the levels of ROS adds another tool in the fight against oxidative tension, a situation all aerobic organisms have to face.

Acknowledgements

This work was supported by Laurentian University and the Northern Ontario Heritage Fund. Azhar Alhasawi is a recipient of the Ministry of Higher Education of Saudi Arabia.

References

Alhasawi A, Auger C, Appanna VP, Chahma MH, Appanna VD. Zinc toxicity and ATP production in *Pseudomonas fluorescens*. J Appl Microbiol 2014;117:65–73.
Appanna VD, Hamel RD, Lévasseur R. The metabolism of aluminum citrate and biosynthesis of oxalic acid in *Pseudomonas fluorescens*. Curr Microbiol 2003;47:32–9.
Beriault R, Hamel R, Chenier D, Mailloux RJ, Joly H, Appanna VD. The overexpression of NADPH-producing enzymes counters the oxidative stress evoked by gallium, an iron mimetic. Biometals 2007;20:165–76.
Bignucolo A, Appanna VP, Thomas SC, Auger C, Han S, Omri A, et al. Hydrogen peroxide stress provokes a metabolic reprogramming in *Pseudomonas fluorescens*: enhanced production of pyruvate. J Biotechnol 2013;167:309–15.
Bradford MM. A rapid and sensitive method for the quantitation of microgram quantities of protein utilizing the principle of protein–dye binding. Anal Biochem 1976;72:248–54.
Bruno-Bárcena JM, Azcárate-Peril MA, Hassan HM. Role of antioxidant enzymes in bacterial resistance to organic acids. Appl Environ Microbiol 2010;76:2747–53.
Campos F, Sobrino T, Ramos-Cabrer P, Castillo J. Oxaloacetate: a novel neuroprotective for acute ischemic stroke. Int J Biochem Cell Biol 2012;44:262–5.
Ezaki B, Gardner RC, Ezaki Y, Matsumoto H. Expression of aluminum-induced genes in transgenic Arabidopsis plants can ameliorate aluminum stress and/or oxidative stress. Plant Physiol 2000;122:657–66.
Grodzinski B, Butt VS. Hydrogen peroxide production and the release of carbon dioxide during glycollate oxidation in leaf peroxisomes. Planta 1976;128:225–31.
Groves MR, Lucana DO. Adaptation to oxidative stress by Gram-positive bacteria: the redox sensing system HbpS-SenS-SenR from *Streptomyces reticuli*. Appl Microbiol Microb Biotechnol 2010;1:33–42.
Habibzadegah-Tari P, Byer KG, Khan SR. Reactive oxygen species mediated calcium oxalate crystal-induced expression of MCP-1 in HK-2 cells. Urol Res 2006;34:26–36.
Hamel R, Appanna VD, Viswanatha T, Puiseux-Dao S. Overexpression of isocitrate lyase is an important strategy in the survival of *Pseudomonas fluorescens* exposed to aluminum. Biochem Biophys Res Commun 2004;317:1189–94.
Hofrichter M, Ziegenhagen D, Vares T, Friedrich M, Jäger MG, Fritsche W, et al. Oxidative decomposition of malonic acid as basis for the action of manganese peroxidase in the absence of hydrogen peroxide. FEBS Lett 1998;434:362–6.
Jozefczak M, Remans T, Vangronsveld J, Cuypers A. Glutathione is a key player in metal-induced oxidative stress defenses. Int J Mol Sci 2012;13:3145–75.
Kohen R, Nyska A. Invited review: oxidation of biological systems: oxidative stress phenomena, antioxidants, redox reactions, and methods for their quantification. Toxicol Pathol 2002;30:620–50.
Lemire J, Milandu Y, Auger C, Bignucolo A, Appanna VP, Appanna VD. Histidine is a source of the antioxidant, α-ketoglutarate, in *Pseudomonas fluorescens* challenged by oxidative stress. FEMS Microbiol Lett 2010;309:170–7.
Lemire J, Appanna VD. Aluminum toxicity and astrocyte dysfunction: a metabolic link to neurological disorders. J Inorg Biochem 2011;105:1513–7.
Li SF, Liu HX, Zhang YB, Yan YC, Li YP. The protective effects of α-ketoacids against oxidative stress on rat spermatozoa *in vitro*. Asian J Androl 2010;12:247–56.
Mailloux RJ, Darwich R, Lemire J, Appanna V. The monitoring of nucleotide diphosphate kinase activity by blue native polyacrylamide gel electrophoresis. Electrophoresis 2008;29:1484–9.
Mailloux RJ, Singh R, Brewer G, Auger C, Lemire J, Appanna VD. α-Ketoglutarate dehydrogenase and glutamate dehydrogenase work in tandem to modulate the antioxidant α-ketoglutarate during oxidative stress in *Pseudomonas fluorescens*. J Bacteriol 2005;191:3804–10.
Mailloux RJ, Bériault R, Lemire J, Singh R, Chénier DR, Hamel RD, et al. The tricarboxylic acid cycle, an ancient metabolic network with a novel twist. PLoS ONE 2007;2:e690.
Mailloux RJ, Lemire J, Appanna VD. Metabolic networks to combat oxidative stress in *Pseudomonas fluorescens*. Antonie van Leeuwenhoek 2011;99:433–42.
Masip L, Veeravalli K, Georgiou G. The many faces of glutathione in bacteria. Antioxid Redox Signal 2006;8:753–62.
Ramsey M, Hartke A, Huycke M. The physiology and metabolism of *Enterococci*. Enterococci 2014;7:1–43.
Sato I, Shimizu M, Hoshino T, Takaya N. The glutathione system of *Aspergillus nidulans* involves a fungus-specific glutathione S-transferase. J Biol Chem 2009;284:8042–53.
Sandoval JM, Arenas FA, Vásquez CC. Glucose-6-phosphate dehydrogenase protects *Escherichia coli* from tellurite-mediated oxidative stress. PLoS ONE 2011;6:e25573.
Sharma P, Jha AB, Dubey RS, Pessarakli M. Reactive oxygen species, oxidative damage, and antioxidative defense mechanism in plants under stressful conditions. J Bot 2012;2012:1–26.
Singh R, Lemire J, Mailloux RJ, Appanna VD. A novel strategy involved anti-oxidative defense: the conversion of NADH into NADPH by a metabolic network. PLoS ONE 2008;3:e2682.

Singh R, Chenier D, Beriault R, Mailloux R, Hamel RD, Appanna VD. Blue native polyacrylamide gel electrophoresis and the monitoring of malate- and oxaloacetate-producing enzymes. J Biochem Biophys Methods 2005;64:189–99.

Somerville GA, Proctor RA. At the crossroads of bacterial metabolism and virulence factor synthesis in *Staphylococci*. Microbiol Mol Biol Rev 2009;73:233–48.

Tannahill GM, Curtis AM, Adamik J, Palsson-McDermott EM, McGettrick AF, Goel G, et al. Succinate is an inflammatory signal that induces IL-1 [bgr] through HIF-1 [agr]. Nature 2013;496:238–42.

Varela-Gomez M, Moreno-Sanchez R, Pardo JP, Perez-Montfort R. Kinetic mechanism and metabolic role of pyruvate phosphate dikinase from *Entamoeba histolytica*. J Biol Chem 2004;279:54124–30.

Ying W. NAD+/NADH and NADP+/NADPH in cellular functions and cell death: regulation and biological consequences. Antioxid Redox Signal 2008;10:179–206.

Yokota A, Kawabata A, Kitaoka S. Mechanism of glyoxylate decarboxylation in the glycolate pathway in *Euglena gracilis* Z participation of Mn^{2+}-dependent NADPH oxidase in chloroplasts. Plant Physiol 1983;71:772–6.

Yokota A, Komura H, Kitaoka S. Refixation of photorespired CO_2 during photosynthesis in *Euglena gracilis* Z. Agric Biol chem 1985;49:3309–10.

Zeller T, Klug G. Detoxification of hydrogen peroxide and expression of catalase genes in *Rhodobacter*. Microbiology 2004;150:3451–62.